

1991

# A Mathematical Model of Electrochemical Reactions Coupled with Homogeneous Chemical Reactions

Ken-Ming Yen

*Texas A & M University - College Station*

Taewhan Yeu

*Texas A & M University - College Station*

Ralph E. White

*University of South Carolina - Columbia, white@cec.sc.edu*

Follow this and additional works at: [https://scholarcommons.sc.edu/eche\\_facpub](https://scholarcommons.sc.edu/eche_facpub)

 Part of the [Chemical Engineering Commons](#)

---

## Publication Info

*Journal of the Electrochemical Society*, 1991, pages 1051-1054.

© The Electrochemical Society, Inc. 1991. All rights reserved. Except as provided under U.S. copyright law, this work may not be reproduced, resold, distributed, or modified without the express permission of The Electrochemical Society (ECS). The archival version of this work was published in the *Journal of the Electrochemical Society*.

<http://www.electrochem.org/>

DOI: 10.1149/1.2085714

<http://dx.doi.org/10.1149/1.2085714>

# A Mathematical Model of Electrochemical Reactions Coupled with Homogeneous Chemical Reactions

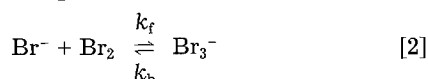
Ken-Ming Yin,\* Taewhan Yeu,\* and Ralph E. White\*\*

Chemical Engineering Department, Texas A&M University, College Station, Texas 77843-3122

The zinc/bromine (Zn/Br<sub>2</sub>) flow battery has received considerable attention in recent years [e.g., (2-4)]. Although it is agreed that the solution chemistry is important in the system, most of the work that has been done is concentrated on the design variables. In this note the basic mass transfer-solution and surface kinetics are studied to furnish a better understanding of the system. The results presented are for electrochemical reaction



coupled with the homogeneous complexation reaction



on a rotating disk electrode (RDE) (4). A detailed discussion of the migration effect is included.

The migration effect for cases without the interference of homogeneous chemical reactions has been discussed thoroughly by Newman (Ref. (5), Chap. 19) and other researchers [e.g., Ref. (6-8)]. Also, Hauser and Newman (9) pointed out the possibility of an interesting potential minimum within the diffusion layer when the supporting electrolyte participates in the electrode reaction without homogeneous chemical reactions involved.

Electrochemical methods have been used for the determination of homogeneous reaction rate constants (10-13). For example, the limiting current density depends on the rate of a homogeneous chemical reaction; Koutecký and Levich (12) analytically derived a limiting current density expression for an electrochemical reaction on a RDE coupled with chemical reactions of the types  $A \rightleftharpoons B$  and  $2A \rightleftharpoons B$ . Also, an experimental determination of the dissociation rate of acetic acid has been done on the RDE by Albery and Bell (Ref. (11), p. 132).

Although analytic analysis has been done, it is shown in this communication that a comprehensive numerical analysis is required to study these systems. For example, the behavior below the limiting current with homogeneous chemical reactions cannot be predicted by any analytic approach, because the electrode kinetics need to be incorporated. Amatore and Saveant (14) numerically investigated the electrochemical, chemical, electrochemical (ECE) and the disproportionation mechanisms. Although electrode kinetics are included, they forcefully set one of the reactant concentrations to zero at the interface, even at the nonlimiting current condition, which is not correct. Yen and Chapman (15) used the orthogonal collocation method for the ECE mechanism and showed that the value of the homogeneous rate constant modifies the limiting current density tremendously. The method they used may save computation time, but accuracy is sacrificed because the chemical reaction occurs close to the interfacial region in which no collocation points are allocated. Adanuvor *et al.* (16) considered the same system as that studied here with the migration effect; however, the bulk concentrations they used do not satisfy the equilibrium condition, which leads to questionable predicted current densities. In this note, this discrepancy is removed. Recently, Hauser and Newman (17) studied the complexation reaction rate of cuprous ions by the singular perturbation method and demonstrated a strategy for the data analysis by lumping relevant variables.

## Theory

For generality, the model equations are developed for multiple reactions, although the studied system is for sin-

\* Electrochemical Society Student Member.

\*\* Electrochemical Society Active Member.

gle electrochemical-chemical reactions. A one-dimensional model is used here, *i.e.*, the model is strictly valid at the center of the RDE. Additional assumptions used are: (i) Dilute solution theory applies, *i.e.*, the driving force for the flux of species is related to the ion-solvent friction. Ion-ion interactions are not considered. (ii) Double-layer charging is not considered. (iii) The solution is isothermal. (iv) The physical and transport parameters are constant within the diffusion layer.

*Governing equations.*—Steady-state mass conservation of species *i* can be written as (Ref. (5), p. 218)

$$0 = -\nabla \cdot \mathbf{N}_i + R_i \quad [3]$$

where  $\mathbf{N}_i$  is the molar flux of species *i* and  $R_i$  is the net generation rate of *i* by homogeneous chemical reactions. For the homogeneous chemical reaction shown in Eq. [2],  $R_{\text{Br}^-} = R_{\text{Br}_2} = -R_{\text{Br}_3^-} = -k_f c_{\text{Br}^-} c_{\text{Br}_2} + k_b c_{\text{Br}_3^-}$ .  $\mathbf{N}_i$  includes migration, diffusion, and convection (Ref. (5), p. 301)

$$\mathbf{N}_i = -z_i u_i F c_i \nabla \Phi - D_i \nabla c_i + \mathbf{v} c_i \quad [4]$$

where the mobility  $u_i$  can be approximated by  $D_i/RT$  according to the Nernst-Einstein relation (Ref. (5), p. 229). For a one-dimensional model, Eq. [3] becomes

$$0 = D_i \frac{d^2 c_i}{dy^2} - v_y \frac{dc_i}{dy} + z_i u_i F \left( c_i \frac{d^2 \Phi}{dy^2} + \frac{dc_i}{dy} \frac{d\Phi}{dy} \right) + R_i \quad [5]$$

The normal velocity at a small distance from the disk surface can be expressed by the first term of a power series approximation

$$v_y = -a\Omega \left( \frac{\Omega}{\nu} \right)^{1/2} y^2 \quad [6]$$

where  $a$  is a constant with the value 0.51023262 (Ref. (5), p. 282),  $\Omega$  is the rotation speed (rad/s), and  $\nu$  is the kinetic viscosity. Also, the solution concentrations of the various species must satisfy the electroneutrality condition

$$0 = \sum_{i=1}^{n_{\text{ion}}} c_i z_i \quad [7]$$

*Boundary conditions.*—The ionic concentrations approach the uniform bulk conditions after a certain characteristic distance or the diffusion layer thickness ( $\delta$ ) from the interface

$$\delta = \left( \frac{3D_R}{av} \right)^{1/3} \left( \frac{\nu}{\Omega} \right)^{1/2} \quad [8]$$

where  $D_R$  represents the diffusivity of the limiting species (Br<sup>-</sup>). It is convenient to set the bulk boundary conditions at  $y = 2\delta$

$$c_i(2\delta) = c_{i,\text{bulk}} \quad [9]$$

where the bulk ionic concentrations satisfy the equilibrium condition ( $K_{\text{eq}} = k_f/k_b = c_{\text{Br}_2,\text{bulk}}/c_{\text{Br}^-,\text{bulk}}c_{\text{Br}_3^-\text{bulk}}$ ) and the electroneutrality condition (Eq. [7]). The solution potential at  $2\delta$  can be assigned an arbitrary constant for convenience; since the value of  $\Phi(2\delta)$  is immaterial, it only serves as a basis of computation (18). Note that these boundary conditions do not include the exact position of the reference electrode ( $y_{\text{RE}}$ ) because the ohmic drop between  $2\delta$  and  $y_{\text{RE}}$  can be easily compensated if the applied current density and specific conductivity of the solution

are known by assuming that Ohm's law ( $i_T = -\kappa d\Phi/dy$ ) applies between  $2\delta$  and  $y_{RE}$ .

The boundary conditions at the electrode surface are that the flux of each ionic species is equal to the associated surface electrochemical reactions

$$-\sum_{j=1}^{nr} \frac{s_{ij} i_j}{n_j F} = N_i \quad [10]$$

where  $N_i = -z_i u_i F c_i d\Phi/dy - D_i dc_i/dy$  at the surface and  $s_{ij}$  is the stoichiometric coefficient of species  $i$  in electrochemical reaction  $j$ . The partial current density  $i_j$  is expressed by the Butler-Volmer equation (18, 19)

$$i_j = i_{0j,ref} \left\{ \prod_i \left( \frac{C_{i,0}}{C_{i,ref}} \right)^{p_{i,j}} \exp \left[ \frac{\alpha_{a,j} n_j F}{RT} (V_d - \Phi_0 - U_{j,ref}) \right] - \prod_i \left( \frac{C_{i,0}}{C_{i,ref}} \right)^{q_{i,j}} \exp \left[ \frac{-\alpha_{c,j} n_j F}{RT} (V_d - \Phi_0 - U_{j,ref}) \right] \right\} \quad [11]$$

The exchange current density  $i_{0j,ref}$  is based on the chosen reference concentrations;  $p_{i,j}$  and  $q_{i,j}$  are the reaction orders for anodic and cathodic reactions. The potential-dependent term,  $V_d - \Phi_0 - U_{j,ref}$ , is the overpotential at the interface for reaction  $j$ , while  $\alpha_{a,j}$  and  $\alpha_{c,j}$  are the corresponding transfer coefficients for anodic and cathodic reactions. The expression  $U_{j,ref}$  is shown in Eq. [8] of Ref. (18). Finally, the electroneutrality condition (Eq. [7]) and the expression of total applied current density

$$i_T = \sum_{j=1}^{nr} i_j \quad [12]$$

serve as the last two equations for the interface solution potential  $\Phi_0$  and the electrode potential  $V_d$ . In this current-controlled model, total current density ( $i_T$ ) rather than the applied potential ( $V_d - \Phi_{RE}$ ) is set.

### Solution Technique

The governing equations and related boundary conditions are cast in the finite difference form. These equations are solved using Newman's BAND subprogram with a matrix solver MATINV (Ref. (5), p. 419). The unknowns determined are ionic concentrations,  $c_i(y)$ , solution potential,  $\Phi(y)$ , and electrode potential,  $V_d$ . The electrode potential,  $V_d$ , which has only a single value at the electrode, is treated as an unknown constant in BAND (6, 7, 19).

### Parameters

The example chosen is the  $\text{Br}^-/\text{Br}_2$  electrode reaction coupled with the tribromide complex reaction in the aqueous solutions. The chemicals introduced into the bulk solution are  $\text{Br}_2$  (0.3 mol/liter) and  $\text{NaBr}$  (0.3 mol/liter). Note the equilibrium bulk concentrations should be calculated based on the equilibrium constant and the amount of chemicals that are added. The associated chemical and electrochemical reactions are shown in Table I. The needed transport data are listed in Table II.

Table I. Electrochemical and chemical reactions.

Electrochemical reaction	$U_j^{\text{th}}$ (V)
$2\text{Br}^- - \text{Br}_2 \rightarrow 2e^-$	1.087 <sup>b</sup>
Electrochemical kinetic parameters	
$\alpha_{a,j}$ $\alpha_{c,j}$ $n_j$ $i_{0j,ref}$ (A/cm <sup>2</sup> )	$U_{j,ref}$ (V)
0.5    0.5    2    0.001861 <sup>c</sup>	1.0466 <sup>d</sup>
Chemical equilibrium    Equilibrium constant (cm <sup>3</sup> /mol)	
$\text{Br}_2 + \text{Br}^- \xrightleftharpoons[k_b]{k_f} \text{Br}_3^-$	$17 \times 10^{28}$

<sup>a</sup> Although the example is for a single electrochemical reaction, the subscript  $j$  is kept for consistency.

<sup>b</sup> Ref. (3).

<sup>c</sup> The exchange current density corresponds to  $c_{i,ref}$  in Ref. (3).

<sup>d</sup> Calculated from Eq. [8] in Ref. (18).

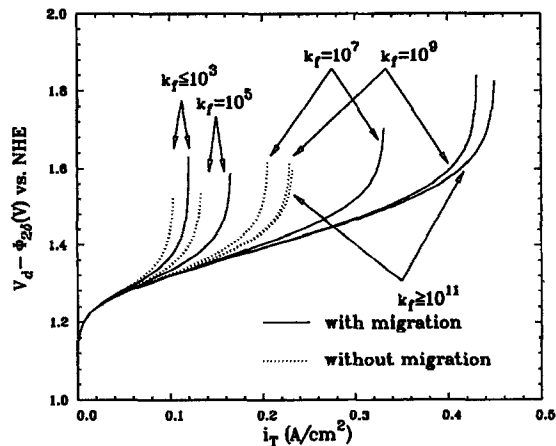


Fig. 1. Polarization curves with different rate constants:  $k_f \leq 10^3$ ,  $= 10^5$ ,  $= 10^7$ ,  $= 10^9$ ,  $\geq 10^{11}$ , from lower to higher current densities.

### Results and Discussion

Figure 1 shows the simulated anodic polarization curves with different homogeneous rate constants. The migration-excluded case is included for comparison, which is done by taking out the migration term in Eq. [5] and by removing the electroneutrality condition (Eq. [7]). For  $k_f \leq 10^3$ , the perturbation of the homogeneous chemical reaction can be neglected so that the polarization curves are the same as those calculated by letting  $R_i = 0$ . It is shown that for  $k_f \geq 10^7$ , the predicted limiting current densities including migration are significantly larger than those without including the migration effect. Obviously, the migration effect is magnified by increasing  $k_f$  (or  $k_b$ ). The concentration profiles within the diffusion layer are shown in Fig. 2a. The much larger  $\text{Br}_2$  concentration at the interface when considering migration reflects the larger limiting current density in Fig. 1. The generally larger predicted current densities when migration is included can be explained by the concentration profiles of  $\text{Br}^-$  and  $\text{Br}_3^-$  being very close to the electrode surface as shown in Fig. 2b. At the interface  $c_{\text{Na}^+} = c_{\text{Br}_3^-}$ , since electroneutrality must be preserved when migration is considered, this causes a higher  $c_{\text{Br}_3^-}$  near the surface. In other words, the anode attracts more negative  $\text{Br}_3^-$  ions to the electrode, which then releases more reactant  $\text{Br}^-$  by the chemical reaction [2] near the electrode compared to the case without migration. Because  $\text{Br}_3^-$  played the role as the supplier of  $\text{Br}^-$ ,  $\text{Br}^-$  has a higher concentration near the electrode when considering migration, and, consequently, has a higher gradient at the interface at the limiting current condition. From the limiting current density at  $k_f = 10^9$  in Fig. 1, it should be clear that the gradient is about twice as much when considering migration compared to the one without considering migration.

An interesting behavior is observed for the electric field ( $E = -d\Phi/dy$ ). As shown in Fig. 3a, the electric field is al-

Table II. Mass transport data.

Species	$z_i$	$D_i^a \times 10^5$	$c_{i,bulk}^b \times 10^3$	$c_{i,ref}^c \times 10^3$
		(cm <sup>2</sup> /s)	(mol/cm <sup>3</sup> )	(mol/cm <sup>3</sup> )
$\text{Na}^+$	1	1.334	0.3	1.0
$\text{Br}^-$	-1	2.084	0.106647	1.08
$\text{Br}_2$	0	1.31	0.106647	0.05
$\text{Br}_3^-$	-1	1.31	0.193353	0.92

$\nu = 0.0123$  cm<sup>2</sup>/s     $T = 298$  K     $\rho_0 = 1.0$  g/cm<sup>3</sup>     $\Omega = 104.7$  rad/s  
 $\delta = 2.23 \times 10^{-3}$  cm

<sup>a</sup>  $D_{\text{Na}^+}$ ,  $D_{\text{Br}^-}$  from Ref. (5), p. 230;  $D_{\text{Br}_2}$ ,  $D_{\text{Br}_3^-}$  from Ref. (3).

<sup>b</sup> The equilibrium bulk concentrations are calculated according to the introduced  $\text{NaBr}$  and  $\text{Br}_2$  concentrations.

<sup>c</sup> The concentrations are from Ref. (3); they correspond to  $i_{0j,ref} = 0.001861$  A/cm<sup>2</sup>.

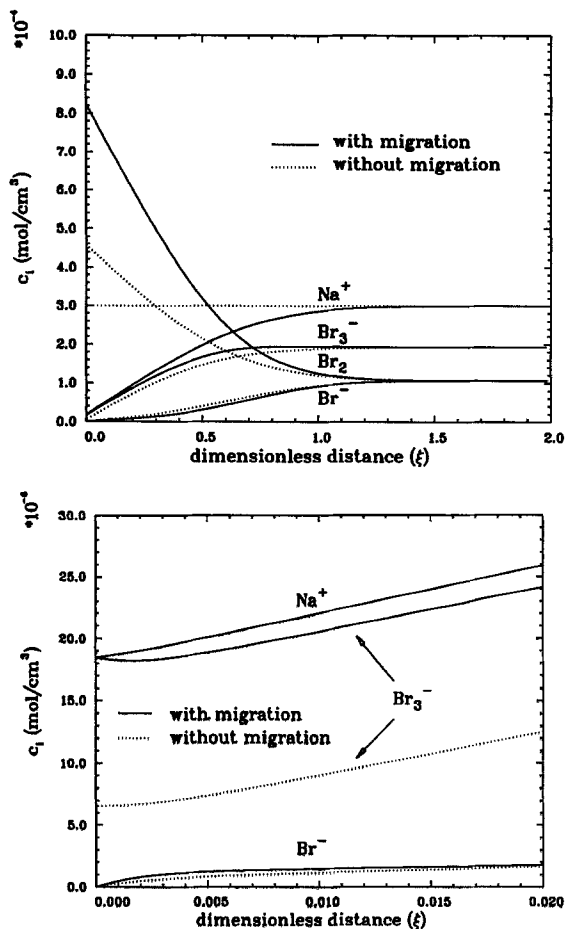


Fig. 2. (a, top) The concentration profiles within the diffusion layer under limiting current density for  $k_f = 10^9$ . (b, bottom) Concentration profiles of  $\text{Na}^+$ ,  $\text{Br}^-$ , and  $\text{Br}_3^-$  close to the electrode under limiting current density for  $k_f = 10^9$ .

most constant near the outer region of the diffusion layer where the concentrations are close to the bulk concentrations. However, higher homogeneous rate constants correspond to higher  $E$  values because of the larger limiting current densities.  $E$  increases rapidly when approaching the electrode because the ionic species are depleted there. There is a maximum in  $E$  close to the electrode as can be seen more clearly in Fig. 3b. Note that the maximum for  $k_f = 10^7$  occurs at  $\xi \approx 0.04$ , as shown in Fig. 3a. Such phenomenon can be explained by the significant difference in concentration gradients in two regions, i.e., the outer diffusion region and the inner chemical reaction region. Figure 4 shows the concentration profiles of  $\text{Br}^-$  within the diffusion layer. It is clear that for  $k_f \neq 10^7$ , a significant difference occurs between the concentration gradients in the two regions. The larger the rate constant, the narrower the inner region (see Fig. 2b for the inner region at  $k_f = 10^9$ ). The total current density, which is constant across the diffusion layer, can be expressed by the respective contributions from Ohm's law and the diffusion current (Ref. (5), p. 221)

$$i_T = -\kappa \frac{d\Phi}{dy} - F \sum_i z_i D_i \frac{dc_i}{dy} \quad [13]$$

where  $\kappa = F^2 \sum_i z_i^2 u_i c_i$ . As shown in Fig. 5a and b, Ohm's law ( $i_{\text{Ohm}} = -\kappa d\Phi/dy$ ) applies well for  $\xi > 1.5$  until the diffusion current ( $i_{\text{Diff}} = -F \sum_i z_i D_i dc_i/dy$ ) becomes important closer to the interface. For  $k_f \leq 10^3$ , when the chemical reaction can be neglected, the diffusion current density (Fig. 5b) increases monotonically toward the electrode because concentration gradients increase steadily when approaching the electrode. As  $k_f$  increases, the diffusion-migration mechanism induced diffusion current is important when  $\xi \leq 1.5$ . Unlike the no-chemical reaction case, there is a drop

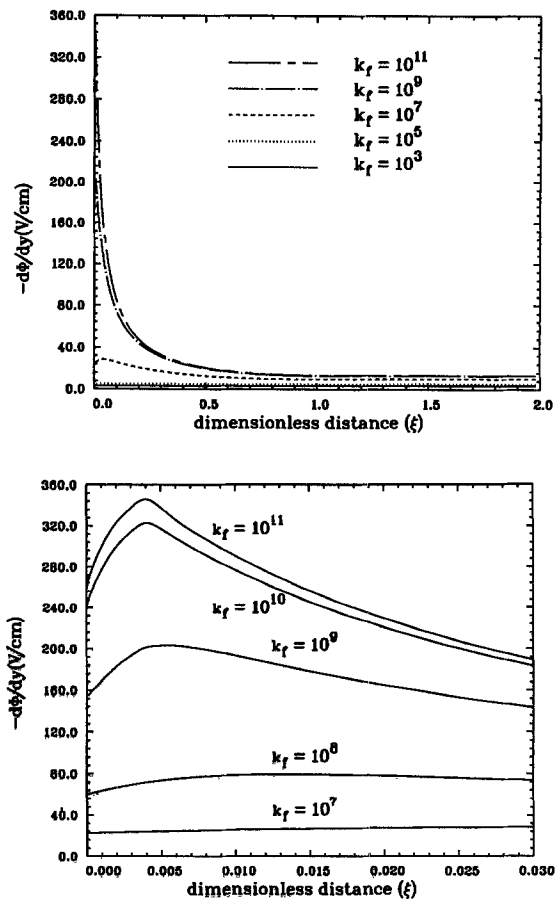


Fig. 3. The potential gradient profiles (a, top) within and (b, bottom) near the diffusion layer at different rate constants under limiting current conditions.

in  $i_{\text{Diff}}$  after a maximum, then  $i_{\text{Diff}}$  increases rapidly near the surface. The drop in  $i_{\text{Diff}}$  must be due to the decrease in the concentration gradients ( $dc_i/dy$ , especially for  $\text{Br}^-$ ), i.e., concentrations in this region are somewhat flattened. The flattening should come from the continuous release of  $\text{Br}^-$  from  $\text{Br}_3^-$ . The flattened concentration region is reflected by the minimum of  $i_{\text{Diff}}$  in Fig. 5b. It should now be clear that  $i_{\text{Diff}}$  will rise again at the interface because of the larger  $dc_{\text{Br}^-}/dy$  there due to the  $\text{Br}^-$  concentration passing through a flattened region and then suddenly dropping to zero at the limiting current condition. Note that for  $k_f = 10^{11}$ , the diffusion current increases after a minimum at  $\xi < 0.005$  which cannot be seen in Fig. 5b. The flattened concentration region and the latter larger concentration gradient at interface characterize the increase and decrease of the potential gradient in Fig. 3b.

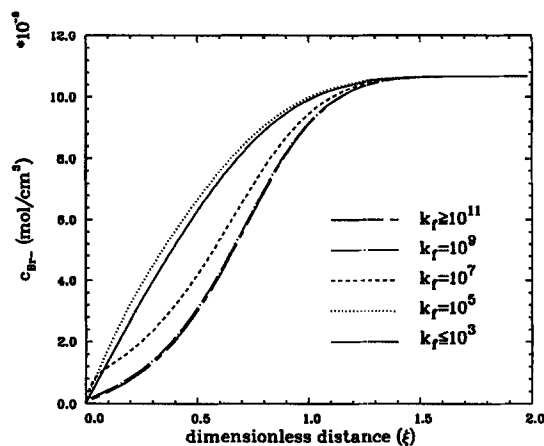


Fig. 4. The  $\text{Br}^-$  concentration profiles within the diffusion layer at various homogeneous rate constants.

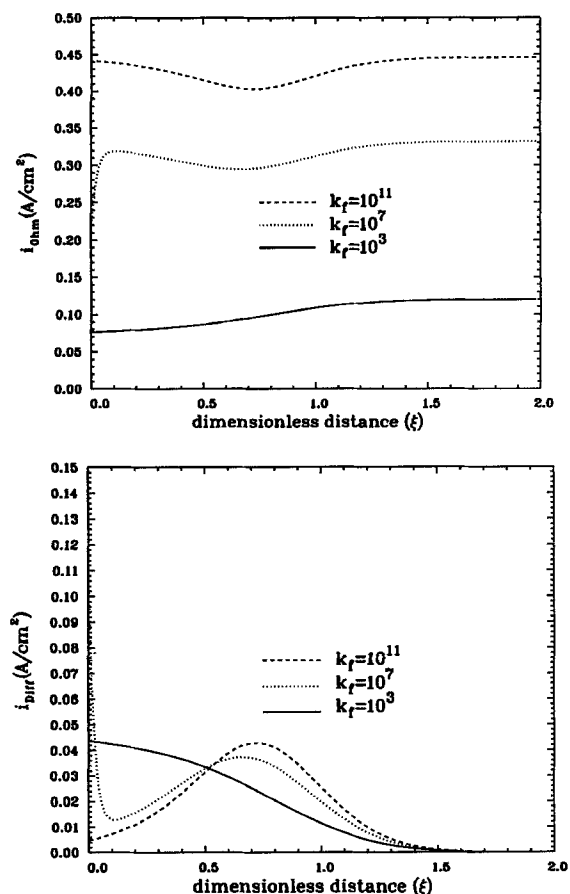


Fig. 5. (a, top) The contribution from ohmic current within the diffusion layer at different rate constants under the limiting current conditions. (b, bottom) The contribution from diffusion current within the diffusion layer at different rate constants under the limiting current conditions.

### Summary

A one-dimensional model of electrochemical reactions coupled with homogeneous chemical reactions is given. An example of the oxidation of  $\text{Br}^-$  coupled with  $\text{Br}^- + \text{Br}_2 \rightleftharpoons \text{Br}_3^-$  shows the importance of including the migration effect. The homogeneous chemical reaction causes a maximum in the electric field within the reaction layer.

### Acknowledgments

The authors are grateful for the support of this project given by Sandia National Laboratories, the Texas Advanced Technology and Research Program, and the Texas A&M University Board of Regents through the Available University Fund.

Manuscript submitted July 23, 1990; revised manuscript received Nov. 30, 1990.

Texas A&M University assisted in meeting the publication costs of this article.

### LIST OF SYMBOLS

$a$	0.51023262
$c_i$	concentration of species $i$ , mol/cm <sup>3</sup>
$c_{i,0}$	concentration of species $i$ at the solid-solution interface, mol/cm <sup>3</sup>
$c_{i,bulk}$	bulk solution concentration of species $i$ , mol/cm <sup>3</sup>
$c_{i,ref}$	reference concentration of species $i$ , mol/cm <sup>3</sup>
$D_i$	diffusion coefficient of species $i$ , cm <sup>2</sup> /s
$D_R$	diffusion coefficient of the limiting species ( $\text{Br}^-$ ), cm <sup>2</sup> /s
$E$	electric field ( $= -d\Phi/dy$ ), V/cm
$F$	Faraday's constant, 96,487 C/mol
$i_j$	partial current density due to reaction $j$ , A/cm <sup>2</sup>
$i_{Diff}$	diffusion current density ( $= -F\sum_{i,z_i} D_i dc_i/dy$ ), A/cm <sup>2</sup>
$i_{Ohm}$	ohmic contribution to total current density ( $= -\kappa d\Phi/dy$ ), A/cm <sup>2</sup>

$i_{0j,ref}$	exchange current density at reference concentrations for reaction $j$ , A/cm <sup>2</sup>
$i_T$	total current density, A/cm <sup>2</sup>
$k_b$	backward homogeneous rate constant, 1/s
$k_f$	forward homogeneous rate constant, cm <sup>3</sup> /s mol
$K_{eq}$	equilibrium constant, cm <sup>3</sup> /mol
$n_{ion}$	number of ionic species
$nr$	number of electrochemical reactions (equal to 1 here)
$n_j$	number of electrons transferred in reaction $j$
$N_i$	flux vector of species $i$ , mol/cm <sup>2</sup> · s
$N_i$	flux of species $i$ in $y$ direction, mol/cm <sup>2</sup> · s
$p_{i,j}$	anodic reaction order of ionic species $i$ in reaction $j$ , dimensionless
$q_{i,j}$	cathodic reaction order of species $i$ in reaction $j$ , dimensionless
$R$	universal gas constant, 8.3143 J/mol · K
$R_i$	the homogeneous reaction rate of species $i$ , mol/s · cm <sup>3</sup>
$s_{ij}$	stoichiometric coefficient of ionic species $i$ in electrochemical reaction $j$ , dimensionless
$T$	absolute temperature, K
$u_i$	mobility of species $i$ ( $= D_i/RT$ ), mol · cm <sup>2</sup> /J · s
$U_{j,ref}$	theoretical open-circuit potential of reaction evaluated at reference concentrations, V
$U_j^\theta$	standard electrode potential for reaction $j$ , V
$\mathbf{v}$	solution velocity vector, cm/s
$v_y$	normal solution velocity, cm/s
$V_d$	potential of the working electrode, V
$y$	normal coordinate, cm
$y_{RE}$	position of reference electrode, cm
$z_i$	charge number of species $i$

### Greek letters

$\alpha_{a,j}$	anodic transfer coefficient for reaction $j$ , dimensionless
$\alpha_{c,j}$	cathodic transfer coefficient for reaction $j$ , dimensionless
$\delta$	characteristic layer thickness according to Eq. [8], cm
$\kappa$	solution conductivity, 1/Ω · cm
$\nu$	kinematic viscosity, cm <sup>2</sup> /s
$\xi$	dimensionless distance ( $= y/\delta$ )
$\rho_0$	pure solvent density, g/cm <sup>3</sup>
$\Phi$	solution potential, V
$\Phi_0$	solution potential adjacent to electrode surface, V
$\Omega$	disk rotation speed, rad/s

### REFERENCES

- J. Lee and J. R. Selman, *This Journal*, **129**, 1670 (1982).
- M. J. Mader and R. E. White, *ibid.*, **133**, 1297 (1986).
- T. I. Evans and R. E. White, *ibid.*, **134**, 866 (1987).
- Yu. V. Pleskov and V. Yu. Filinovskii, "The Rotating Disc Electrode," Consultants Bureau, New York (1976).
- J. S. Newman, "Electrochemical Systems," Prentice Hall, Inc., Englewood Cliffs, NJ (1973).
- S. Chen, K.-M. Yin, and R. E. White, *This Journal*, **135**, 2193 (1988).
- K.-M. Yin and R. E. White, *AIChE J.*, **36**, 187 (1990).
- C. Y. Mak and H. Y. Cheh, *This Journal*, **135**, 2262 (1988).
- A. K. Hauser and J. Newman, *ibid.*, **136**, 3320 (1989).
- E. F. Caldin, "Fast Reactions in Solutions," John Wiley and Sons, New York (1964).
- J. Albery, "Electrode Kinetics," Clarendon Press, Oxford (1975).
- V. G. Levich, "Physicochemical Hydrodynamics," Prentice Hall, Inc., Englewood Cliffs, NJ (1962).
- A. J. Bard and L. R. Faulkner, "Electrochemical Methods: Fundamentals and Applications," John Wiley and Sons, New York (1980).
- C. Amatore and J. M. Saveant, *J. Electroanal. Chem.*, **85**, 27 (1977).
- S.-C. Yen and T. W. Chapman, *Chem. Eng. Commun.*, **38**, 159 (1985).
- P. K. Adanuvor, R. E. White, and S. E. Lorimer, *This Journal*, **134**, 1450 (1987).
- A. K. Hauser and J. Newman, *This Journal*, **136**, 3250 (1989).
- R. E. White, S. E. Lorimer, and R. Darby, *ibid.*, **130**, 1123 (1983).
- R. E. White, Ph.D. Thesis, University of California at Berkeley (1977).